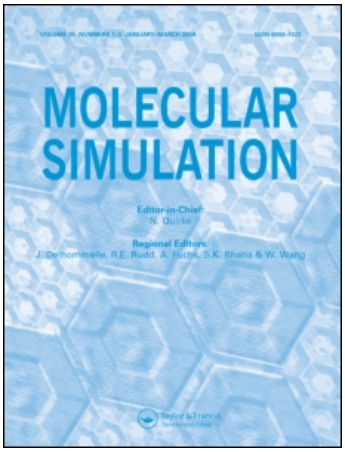

Molecular Simulation
Publication details, including instructions for authors and subscription information:
http://www.informaworld.com/smpp/title~content=t713644482

Shear Viscosity of Model Mixtures by Nonequilibrium Molecular Dynamics III. Effect of Quadrupolar Interactions

Song Hi Lee[a]; Peter T. Cummings[bc]
[a] Department of Chemistry, Kyungsung University, Pusan, Korea [b] Departments of Chemical Engineering, Chemistry and Computer Science, University of Tennessee, Knoxville, TN, USA [c] Chemical Technology Division, Oak Ridge National Laboratory, Oak Ridge, TN, USA

To cite this Article Lee, Song Hi and Cummings, Peter T.(2001) 'Shear Viscosity of Model Mixtures by Nonequilibrium Molecular Dynamics III. Effect of Quadrupolar Interactions', Molecular Simulation, 27: 2, 115 — 137
To link to this Article: DOI: 10.1080/08927020108023127
URL: http://dx.doi.org/10.1080/08927020108023127

Molecular Simulation, 2001, Vol. 27, pp. 115–137
Reprints available directly from the publisher
Photocopying permitted by license only

SHEAR VISCOSITY OF MODEL MIXTURES BY NONEQUILIBRIUM MOLECULAR DYNAMICS. III. EFFECT OF QUADRUPOLAR INTERACTIONS

SONG HI LEE[a,*] and PETER T. CUMMINGS[b]

[a]*Department of Chemistry, Kyungsung University, Pusan 608-736, Korea;*
[b]*Departments of Chemical Engineering, Chemistry and Computer Science, University of Tennessee, Knoxville, TN 37996-2200, USA and Chemical Technology Division, Oak Ridge National Laboratory, Oak Ridge, TN 37831-6268, USA*

(Received September 2000; accepted September 2000)

We present new results for thermodynamic properties and viscosities of pure quadrupolar fluids, a pure dipolar quadrupolar fluid, nonquadrupolar/quadrupolar mixtures, and quadrupolar/quadrupolar mixtures. It is evident that, the addition of quadrupolar interactions to the pure Ar and the addition of quadrupolar interactions to the pure dipolar Ar, leads to higher viscosities as was observed in the addition of dipolar interactions to the pure Ar [Lee and Cummings, *J. Chem. Phys.*, **105**, 2044 (1996)]. The total energies and the mixture densities show a linear dependence for both nonquadrupolar Ar/quadrupolar Kr (case B) and quadrupolar Ar/quadrupolar Kr (case C), and the linearity of case C is better than that of case B. This is not consistent with the idea that in the cases of the dipolar mixtures, dipolar/dipolar and nondipolar/nondipolar mixture are likely to be more ideal than nondipolar/dipolar mixtures. This is mainly due to the weaker interaction of quadrupole–quadrupole than that of dipole–dipole.

Keywords: Shear viscosities; Quadrupoles; Nonequilibrium

I. INTRODUCTION

In previous papers [1–3], we reported non-equilibrium molecular dynamics (NEMD) calculations of shear viscosities of pure argon and krypton liquids

*Corresponding author.

TABLE I Pure systems and mixtures studied in a series of our NEMD simulations*

Systems	*Pure*	*Kr*	*Kr+D*	*Kr+Q*
pure		I	II	III
Ar	I	I	II	III
Ar+*D*	II		II	
Ar+*Q*	III			III
Ar+*D*+*Q*	III			
Ar+Q^++Q^-	III			

*I: paper I (Ref. [1]), II: paper II (Ref. [3]), and III: this paper.

using Lennard-Jones (LJ) and Barker-Fisher Watts (BFW) potentials [4, 5] without considering a three-body potential, and argon/krypton mixtures using LJ potential [1], pure argon liquid using the highly accurate BFW model both with and without the Axilrod-Teller [6] three-body potential [2], and pure dipolar fluids, nondipolar/dipolar fluid mixtures, and dipolar/dipolar fluid mixtures using LJ plus Stockmayer [7] potentials [3]. Continuing those studies here, we discuss new results for thermodynamic properties and viscosities of pure quadrupolar fluids, pure dipolar quadrupolar fluid, nonquadrupolar/quadrupolar mixtures, and quadrupolar/quadrupolar mixtures. By comparing the computed shear viscosity with those from earlier studies, the effect of quadrupolar interactions on shear viscosity can be evaluated. Table I summarizes the pure systems and mixtures studied in the previous and present papers.

In Section II, we present the brief intermolecular potentials and NEMD algorithm used to calculate the shear viscosity. The results of our simulations are discussed in Section III.

II. SIMULATION DETAILS

In this section, we describe the intermolecular potentials and the briefs of the NEMD simulation algorithm.

II.1. Intermolecular Potentials

For the study of properties of pure quadrupolar fluids, pure dipolar quadrupolar fluid, nonquadrupolar/quadrupolar mixtures, and quadrupolar/quadrupolar mixtures, the following potential is used:

$$u_{ij}(\mathbf{r}, \mathbf{e}_i, \mathbf{e}_j) = 4\,\varepsilon_{ij}\left[\left(\frac{\sigma_{ij}}{r}\right)^{12} - \left(\frac{\sigma_{ij}}{r}\right)^{6}\right] + u_{ij}^{DD} + u_{ij}^{DQ} + u_{ij}^{DQ} \qquad (1)$$

where $\mathbf{r}=\mathbf{r}_{ij}=\mathbf{r}_i-\mathbf{r}_j$ is the vector joining the centers of particles i and j, $r=|\mathbf{r}|$, $\mathbf{e}_i$ is the orientational unit vector of molecule i, ε_{ij} and σ_{ij} are the LJ parameters. u_{ij}^{DD} is the dipole–dipole potential which is given in Ref. [3] in detail, u_{ij}^{DQ} is the dipole–quadrupole potential:

$$u_{ij}^{DQ}(\mathbf{r},\mathbf{e}_i,\mathbf{e}_j)=\frac{3}{2}\mu_i Q_j\left[-\frac{(\mathbf{r}\cdot\mathbf{e}_i)}{r^5}+\frac{5(\mathbf{r}\cdot\mathbf{e}_i)(\mathbf{r}\cdot\mathbf{e}_j)^2}{r^7}-\frac{2(\mathbf{r}\cdot\mathbf{e}_j)(\mathbf{e}_i\cdot\mathbf{e}_j)}{r^5}\right]$$
$$+\frac{3}{2}\mu_j Q_i\left[\frac{(\mathbf{r}\cdot\mathbf{e}_j)}{r^5}-\frac{5(\mathbf{r}\cdot\mathbf{e}_j)(\mathbf{r}\cdot\mathbf{e}_i)^2}{r^7}+\frac{2(\mathbf{r}\cdot\mathbf{e}_i)(\mathbf{e}_i\cdot\mathbf{e}_j)}{r^5}\right] \quad (2)$$

and u_{ij}^{QQ} is the quadrupole–quadrupole potential:

$$u_{ij}^{QQ}(\mathbf{r},\mathbf{e}_i,\mathbf{e}_j)=\frac{3}{4}Q_iQ_j\left[\frac{1}{r^5}-\frac{5(\mathbf{r}\cdot\mathbf{e}_i)^2}{r^7}-\frac{5(\mathbf{r}\cdot\mathbf{e}_j)^2}{r^7}-\frac{15(\mathbf{r}\cdot\mathbf{e}_i)^2(\mathbf{r}\cdot\mathbf{e}_j)^2}{r^9}\right]$$
$$+\frac{3}{2}Q_iQ_j\left[\frac{(\mathbf{e}_i\cdot\mathbf{e}_j)}{r^{5/2}}-\frac{2(\mathbf{r}\cdot\mathbf{e}_i)(\mathbf{r}\cdot\mathbf{e}_j)}{r^{9/2}}\right]^2 \quad (3)$$

where μ_i and Q_i are the magnitudes of dipole and quadrupole moments of molecule i, respectively. The dipole and quadrupole moments are given in the units of D (Debye, $1\,\mathrm{D}=10^{-18}\,\mathrm{cm}^{3/2}\,\mathrm{erg}^{1/2}$) B (Buckingham, $1\,\mathrm{B}=10^{-26}\,\mathrm{cm}^{5/2}\,\mathrm{erg}^{1/2}$). The dipole–quadrupole and quadrupole–quadrupole forces and torques on molecule i due to molecule j may be written as

$$\mathbf{F}_{ij}^{DQ}(\mathbf{r},\mathbf{e}_i,\mathbf{e}_j)=\frac{3}{2}\mu_i Q_j\left[-\frac{5\mathbf{r}(\mathbf{r}\cdot\mathbf{e}_i)}{r^7}+\frac{\mathbf{e}_i}{r^5}+\frac{35\mathbf{r}(\mathbf{r}\cdot\mathbf{e}_i)(\mathbf{r}\cdot\mathbf{e}_j)^2}{r^9}-\frac{5\mathbf{e}_i(\mathbf{r}\cdot\mathbf{e}_j)^2}{r^5}\right.$$
$$\left.-\frac{10(\mathbf{r}\cdot\mathbf{e}_i)(\mathbf{r}\cdot\mathbf{e}_j)\mathbf{e}_j}{r^7}+\frac{10(\mathbf{r}\cdot\mathbf{e}_j)(\mathbf{e}_i\cdot\mathbf{e}_j)}{r^7}+\frac{2\mathbf{e}_j(\mathbf{e}_i\cdot\mathbf{e}_j)}{r^5}\right]$$
$$+\frac{3}{2}\mu_j Q_i\left[\frac{5\mathbf{r}(\mathbf{r}\cdot\mathbf{e}_j)}{r^7}-\frac{\mathbf{e}_j}{r^5}-\frac{35\mathbf{r}(\mathbf{r}\cdot\mathbf{e}_j)(\mathbf{r}\cdot\mathbf{e}_i)^2}{r^9}+\frac{5\mathbf{e}_j(\mathbf{r}\cdot\mathbf{e}_i)^2}{r^5}\right.$$
$$\left.+\frac{10(\mathbf{r}\cdot\mathbf{e}_i)(\mathbf{r}\cdot\mathbf{e}_j)\mathbf{e}_i}{r^7}-\frac{10(\mathbf{r}\cdot\mathbf{e}_i)(\mathbf{e}_i\cdot\mathbf{e}_j)}{r^7}-\frac{2\mathbf{e}_i(\mathbf{e}_i\cdot\mathbf{e}_j)}{r^5}\right] \quad (4)$$

$$\mathbf{T}_{ij}^{DQ}(\mathbf{r},\mathbf{e}_i,\mathbf{e}_j)=\frac{3}{2}\mu_i Q_j\left[\frac{(\mathbf{e}_i\times\mathbf{r})}{r^5}-\frac{5(\mathbf{e}_i\times\mathbf{r})(\mathbf{r}\cdot\mathbf{e}_j)^2}{r^7}+\frac{2(\mathbf{r}\cdot\mathbf{e}_j)(\mathbf{e}_i\times\mathbf{e}_j)}{r^5}\right]$$
$$+\frac{3}{2}\mu_j Q_i\left[\frac{10(\mathbf{r}\cdot\mathbf{e}_i)(\mathbf{r}\cdot\mathbf{e}_j)(\mathbf{e}_i\times\mathbf{r})}{r^7}-\frac{2(\mathbf{e}_i\times\mathbf{r})(\mathbf{e}_i\cdot\mathbf{e}_j)}{r^5}\right.$$
$$\left.-\frac{2(\mathbf{r}\cdot\mathbf{e}_i)(\mathbf{e}_i\times\mathbf{e}_j)}{r^5}\right] \quad (5)$$

$$\mathbf{F}_{ij}^{QQ}(\mathbf{r},\mathbf{e}_i,\mathbf{e}_j) = \frac{15}{4}Q_iQ_j\left[\frac{\mathbf{r}}{r^7} - \frac{7\mathbf{r}(\mathbf{r}\cdot\mathbf{e}_i)^2}{r^9} + \frac{2(\mathbf{r}\cdot\mathbf{e}_i)\mathbf{e}_i}{r^7} - \frac{7\mathbf{r}(\mathbf{r}\cdot\mathbf{e}_j)^2}{r^9} + \frac{2(\mathbf{r}\cdot\mathbf{e}_j)\mathbf{e}_j}{r^7} - \frac{27\mathbf{r}(\mathbf{r}\cdot\mathbf{e}_i)^2(\mathbf{r}\cdot\mathbf{e}_j)^2}{r^{11}} + \frac{6(\mathbf{r}\cdot\mathbf{e}_i)(\mathbf{r}\cdot\mathbf{e}_j)^2\mathbf{e}_i}{r^9} + \frac{6(\mathbf{r}\cdot\mathbf{e}_j)(\mathbf{r}\cdot\mathbf{e}_i)^2\mathbf{e}_j}{r^9}\right] + \frac{15}{2}Q_iQ_j\left[\frac{(\mathbf{e}_i\cdot\mathbf{e}_j)}{r^{5/2}} - \frac{5(\mathbf{r}\cdot\mathbf{e}_i)(\mathbf{r}\cdot\mathbf{e}_j)}{r^{9/2}}\right]\left[\frac{(\mathbf{e}_i\cdot\mathbf{e}_j)\mathbf{r}}{r^{9/2}} - \frac{9(\mathbf{r}\cdot\mathbf{e}_i)(\mathbf{r}\cdot\mathbf{e}_j)\mathbf{r}}{r^{13/2}} + \frac{2(\mathbf{r}\cdot\mathbf{e}_i)\mathbf{e}_j}{r^{9/2}} + \frac{2(\mathbf{r}\cdot\mathbf{e}_j)\mathbf{e}_i}{r^{9/2}}\right] \tag{6}$$

$$\mathbf{T}_{ij}^{QQ}(\mathbf{r},\mathbf{e}_i,\mathbf{e}_j) = \frac{3}{4}Q_iQ_j\left[\frac{10(\mathbf{r}\cdot\mathbf{e}_i)(\mathbf{e}_i\times\mathbf{r})}{r^7} + \frac{30(\mathbf{r}\cdot\mathbf{e}_i)(\mathbf{r}\cdot\mathbf{e}_j)^2(\mathbf{e}_i\times\mathbf{r})}{r^9}\right] - 3Q_iQ_j\left[\frac{(\mathbf{e}_i\cdot\mathbf{e}_j)}{r^{5/2}} - \frac{5(\mathbf{r}\cdot\mathbf{e}_i)(\mathbf{r}\cdot\mathbf{e}_j)}{r^{9/2}}\right]\left[\frac{(\mathbf{e}_i\times\mathbf{e}_j)}{r^{5/2}} - \frac{5(\mathbf{r}\cdot\mathbf{e}_i)(\mathbf{e}_j\times\mathbf{r})}{r^{9/2}}\right] \tag{7}$$

The corresponding dipole–dipole force and torque are given in Ref. [3] in detail. The LJ parameters are given in Table II and are the same as those used in Ref. [1] for liquid argon and krypton. The cross interaction parameters for the LJ interactions are obtained from the simple Lorentz-Berthelot rules.

II.2. NpT NEMD Algorithm

For the dipolar quadrupolar fluid mixtures, the NEMD algorithm used in this paper is the mixture version of the isokinetic sllod algorithm used in the previous paper [3]. The equations of motion for this algorithm are given by

$$\frac{d\mathbf{r}_i}{dt} = \frac{\mathbf{p}_i}{m_i} + \mathbf{r}_i\cdot\nabla\mathbf{u} + \kappa'\mathbf{r}_i \tag{8a}$$

$$\frac{d\mathbf{p}_i}{dt} = \mathbf{F}_i - \mathbf{p}_i\cdot\nabla\mathbf{u} - \kappa'\mathbf{p}_i - \alpha\mathbf{p}_i \tag{8b}$$

TABLE II LJ parameters for Ar/Ar, Kr/Kr, and Ar/Kr interactions

Interaction	$\sigma(A)$	$\varepsilon/k_B(^\circ K)$
Ar/Ar	3.405	119.8
Kr/Kr	3.633	167.0
Ar/Kr	3.519	141.4

$$\mathbf{T}_i p = \mathbf{A}_i \mathbf{T}_i \tag{9a}$$

$$\frac{d\mathbf{L}_i p}{dt} = \mathbf{T}_i p \tag{9b}$$

$$\omega_i p = L_i p / \mathbf{I}_i, \tag{9c}$$

$$\frac{d}{dt}\begin{pmatrix} q_{i1} \\ q_{i2} \\ q_{i3} \\ q_{i4} \end{pmatrix} = \frac{1}{2}\begin{pmatrix} -q_{i3} & -q_{i4} & q_{i2} & q_{i1} \\ q_{i4} & -q_{i3} & -q_{i1} & q_{i2} \\ q_{i1} & q_{i2} & q_{i4} & q_{i3} \\ -q_{i2} & q_{i1} & -q_{i3} & q_{i4} \end{pmatrix}\begin{pmatrix} w_{ix^p} \\ w_{iy^p} \\ 0 \\ 0 \end{pmatrix} \tag{9d}$$

$$\begin{aligned}
A_{i11} &= -q_{i1}q_{i1} + -q_{i2}q_{i2} - q_{i3}q_{i3} + q_{i4}q_{i4} \\
A_{i12} &= 2(q_{i3}q_{i4} - q_{i1}q_{i2}) \\
A_{i13} &= 2(q_{i2}q_{i3} + q_{i1}q_{i4}) \\
A_{i21} &= -2(q_{i1}q_{i2} + q_{i3}q_{i4}) \\
A_{i22} &= q_{i1}q_{i1} - q_{i2}q_{i2} - q_{i3}q_{i3} + q_{i4}q_{i4} \\
A_{i23} &= 2(q_{i2}q_{i4} - q_{i1}q_{i3}) \\
A_{i31} &= 2(q_{i2}q_{i3} - q_{i1}q_{i4}) \\
A_{i32} &= -2(q_{i1}q_{i3} + q_{i2}q_{i4}) \\
A_{i33} &= -q_{i1}q_{i1} - q_{i2}q_{i2} + q_{i3}q_{i3} + q_{i4}q_{i4}
\end{aligned} \tag{9e}$$

In Eqs. (8a) and (8b), $\mathbf{r}_i$, m_i, and $\mathbf{p}_i$ are the position, mass, and momentum respectively of molecule i, $\mathbf{F}_i$ is the force exerted by the other molecules on molecule i, $\mathbf{u} = (u_x, 0, 0)$ with $u_x = \gamma y$ is the velocity field corresponding to planar Couette flow. In Eqs. (9a)–(9e), $\mathbf{L}_i$ is the angular momentum of molecule i and $\mathbf{T}_i$ is the torque on molecule i in the laboratory frame, the superscript p denotes a quantity in the principal axis frame of a molecule, $\mathbf{A}_i$ is the rotation matrix which transforms vectors from the laboratory frame to the principal axis frame of molecule i, the elements of $\mathbf{A}_i$ are given by Eq. (9e), $\mathbf{I}_i$ is the moment of inertia of molecule i and $q_{i\alpha}(\alpha = 1, 2, 3, 4)$ are the quaternion parameters related to the Euler angles describing the orientation of molecule i in the laboratory frame

$$e_{ix} = 2(q_{i2}q_{i3} - q_{i1}q_{i4}) \tag{10a}$$

$$e_{iy} = -2(q_{i1}q_{i3} + q_{i2}q_{i4}) \tag{10b}$$

$$e_{iz} = -q_{i1}q_{i1} - q_{i2}q_{i2} + q_{i3}q_{i3} + q_{i4}q_{i4} \tag{10c}$$

where $e_{i\alpha}(\alpha = x, y, z)$ are the components of is the orientational unit vector of molecule i. Note that the quaternions satisfy the normalization $q_{i1}^2 + q_{i2}^2 + q_{i3}^2 + q_{i4}^2 = 1$. The use of quaternions lead to singularity free equations of motion [8, 9]. The parameter α is the thermostating constant, given by

$$\alpha = \frac{\sum_{i=1}^{N}[(\mathbf{p}_i \cdot \mathbf{F}_i - \gamma p_{ix} p_{iy})/m_i]}{\sum_{i=1}^{N}[(\mathbf{p}_i \cdot \mathbf{p}_i)/m_i]} - \dot{\kappa} \tag{11}$$

The effect of the thermostating term involving $\alpha \mathbf{p}_i$ in Eq. (8b) is to hold the translational kinetic energy constant. The functional form of this term is derived by Gauss's principle of least constraint. The momenta in Eqs. (9a) and (9b) are measured with respect to the streaming velocity of the fluid and are known as peculiar momenta. In similar fashion to the thermostating constant, the dilation rate $\kappa' = d\kappa/dt$ controls the volume of the system in order to constrain the pressure p. If $\kappa' = 0$, the equations of motion are at constant volume (isochoric) rather than at constant pressure (isobaric). The pressure is the trace of the pressure tensor $\mathbf{P}$, which is expressed in terms of molecular quantity by

$$\mathbf{P}V = \sum_{i=1}^{N} \mathbf{p}_i \mathbf{p}_i / m_i + \sum_{1 < i < j < N} \mathbf{r}_{ij} \mathbf{F}_{ij} \tag{12}$$

where V is the volume of the system and $\mathbf{F}_{ij}$ is the force between molecules i and j. The equation of motion for the dilation rate for a pure fluid is given by Hood *et al.* [10]. The extension to mixtures of fluids with anisotropic interactions is straightforward and given by

$$\kappa' = \frac{\sum_{1 < i < j < N}\{\mathbf{H}_{ij} \cdot [(\mathbf{p}_i/m_i) - (\mathbf{p}_j/m_j)] + \gamma H_{xij} y_{ij}\}}{9pV - \sum_{1 < i < j < N} \mathbf{H}_{ij} \cdot \mathbf{r}_{ij}} \tag{13}$$

where H_{xij} is the x component of $\mathbf{H}_{ij}$,

$$\mathbf{H}_{ij} = \mathbf{F}_{ij} + \mathbf{r}_{ij} \cdot \left(\frac{d\mathbf{F}_{ij}}{d\mathbf{r}_{ij}} \right) \tag{14}$$

For the dipole–quadrupole and quadrupole–quadrupole potentials, we have

$$\mathbf{H}_{ij}^{DQ}(\mathbf{r}, \mathbf{e}_i, \mathbf{e}_j) = \frac{3}{2} \mu_i \, Q_j \left[\frac{25\mathbf{r}(\mathbf{r} \cdot \mathbf{e}_i)}{r^7} - \frac{9\mathbf{e}_i}{r^5} - \frac{245\mathbf{r}(\mathbf{r} \cdot \mathbf{e}_i)(\mathbf{r} \cdot \mathbf{e}_j)^2}{r^9} + \frac{65\mathbf{e}_i(\mathbf{r} \cdot \mathbf{e}_j)^2}{r^5} \right.$$
$$\left. + \frac{100(\mathbf{r} \cdot \mathbf{e}_i)(\mathbf{r} \cdot \mathbf{e}_j)\mathbf{e}_j}{r^7} + \frac{50(\mathbf{r} \cdot \mathbf{e}_i)(\mathbf{e}_i \cdot \mathbf{e}_j)}{r^7} - \frac{18\mathbf{e}_j(\mathbf{e}_i \cdot \mathbf{e}_j)}{r^5} \right]$$

$$-\frac{3}{2}\mu_j Q_i\left[\frac{25\mathbf{r}(\mathbf{r}\cdot\mathbf{e}_j)}{r^7}-\frac{9\mathbf{e}_j}{r^5}\right.$$
$$-\frac{245\mathbf{r}(\mathbf{r}\cdot\mathbf{e}_j)(\mathbf{r}\cdot\mathbf{e}_i)^2}{r^9}+\frac{65\mathbf{e}_j(\mathbf{r}\cdot\mathbf{e}_i)^2}{r^5}$$
$$+\frac{100(\mathbf{r}\cdot\mathbf{e}_i)(\mathbf{r}\cdot\mathbf{e}_j)\mathbf{e}_i}{r^7}+\frac{50(\mathbf{r}\cdot\mathbf{e}_i)(\mathbf{e}_i\cdot\mathbf{e}_j)}{r^7}$$
$$\left.-\frac{18\mathbf{e}_i(\mathbf{e}_i\cdot\mathbf{e}_j)}{r^5}\right] \tag{15}$$

$$\mathbf{H}_{ij}^{DQ}\cdot\mathbf{r}_{ij}=-16u_{ij}^{DQ} \tag{16}$$

$$\mathbf{H}_{ij}^{QQ}(\mathbf{r},\mathbf{e}_i,\mathbf{e}_j)=-\frac{15}{4}Q_iQ_j\left[\frac{5\mathbf{r}}{r^7}-\frac{49\mathbf{r}(\mathbf{r}\cdot\mathbf{e}_i)^2}{r^9}\right.$$
$$+\frac{24(\mathbf{r}\cdot\mathbf{e}_i)\mathbf{e}_i}{r^7}-\frac{49\mathbf{r}(\mathbf{r}\cdot\mathbf{e}_j)^2}{r^9}+\frac{24(\mathbf{r}\cdot\mathbf{e}_j)\mathbf{e}_j}{r^7}$$
$$-\frac{243\mathbf{r}(\mathbf{r}\cdot\mathbf{e}_i)^2(\mathbf{r}\cdot\mathbf{e}_j)^2}{r^{11}}+\frac{84(\mathbf{r}\cdot\mathbf{e}_i)(\mathbf{r}\cdot\mathbf{e}_j)^2\mathbf{e}_i}{r^9}$$
$$\left.+\frac{84(\mathbf{r}\cdot\mathbf{e}_j)(\mathbf{r}\cdot\mathbf{e}_i)^2\mathbf{e}_j}{r^9}\right]$$
$$-\frac{75}{2}Q_iQ_j\left[\frac{(\mathbf{e}_i\cdot\mathbf{e}_j)\mathbf{r}}{r^{9/2}}-\frac{49(\mathbf{r}\cdot\mathbf{e}_i)(\mathbf{r}\cdot\mathbf{e}_j)\mathbf{r}}{r^{13/2}}\right.$$
$$\left.+\frac{2(\mathbf{r}\cdot\mathbf{e}_i)\mathbf{e}_j}{r^{9/2}}+\frac{2(\mathbf{r}\cdot\mathbf{e}_j)\mathbf{e}_i}{r^{9/2}}\right]\left[\frac{(\mathbf{e}_i\cdot\mathbf{e}_j)}{r^{5/2}}-\frac{5(\mathbf{r}\cdot\mathbf{e}_i)(\mathbf{re}_j)}{r^{9/2}}\right] \tag{17}$$

and

$$\mathbf{H}_{ij}^{QQ}\cdot\mathbf{r}_{ij}=-25u_{ij}^{QQ} \tag{18}$$

Derivation of Eqs. (15) and (17) can be checked by Eqs. (16) and (18) which have the following form $\mathbf{H}_{ij}\cdot\mathbf{r}_{ij}=-n^2\,u_{ij}$ where n is found in $u_{ij}\propto(1/r_{ij})^n$. The same form is found in the corresponding dipole–dipole expressions in Ref. [3].

These equations of motion are combined with the Lees-Edwards "sliding brick" boundary conditions [11]. In the absence of the thermostat and the isobaric constraint, the terms in Eqs. (8a) and (8b) involving the strain field, $\nabla\mathbf{u}$, cancel to yield Newton's equations of motion relating $\mathbf{r}_i$ and $\mathbf{F}_i$. This implies that the sllod algorithm truly generates boundary driven planar Couette flow, leading to the conclusion that it is correct to arbitrary order in the strain rate [12]. In order to obtain a good signal-to-noise ratio, with

NEMD it is necessary to use strain rates γ which are high enough to cause the shear viscosity to be strain rate dependent. In order to compute the shear viscosity of a Newtonian fluid using the sllod algorithm, after the simulation reaches the steady state at a given strain rate γ one computes and averages the pressure tensor defined in Eq. (12). The strain rate dependent shear viscosity is then obtained from Newton's law of viscosity

$$\eta = \frac{p_{xy} + p_{yx}}{2\gamma} \tag{19}$$

where p_{xy} and p_{yx} are the averaged xy and yx components of **P**. From kinetic and mode coupling theories, it is known [13–15] that to leading order the strain rate dependence of the shear viscosity is linear in $\gamma^{1/2}$. Hence, to apply the sllod algorithm to a Newtonian fluid, one performs several simulations at differing strain rates g and fits the resulting strain dependent viscosities to the equation

$$\eta = \eta(0) + \eta_1 \gamma^{1/2} \tag{20}$$

The zero strain rate extrapolation of η, $\eta(0)$, is thus the Newtonian viscosity.

II.3. Simulation Systems

As indicated in Table I, the simulation systems which we performed were (1) pure quadrupolar argon, (2) pure quadrupolar krypton, (3) pure dipolar quadrupolar argon, (4) mixture of two kinds of quadrupolar argon, (5) mixture of nonquadrupolar argon and quadrupolar krypton, and (6) mixture of quadrupolar argon and quadrupolar krypton. All simulations were carried on 108 molecules fully equilibrated for at least 300,000 time steps of 10^{-15} second(1 fs). The intermolecular potentials were subject to spherical cutoffs as follows: the cutoff distance was $2.25\sigma_{Ar}$ for pure quadrupolar Ar, and $2.25\sigma_{Kr}$ for pure fluids and mixtures containing quadrupolar Kr.

III. RESULTS

The results are summarized in Table III for the pure quadrupolar Ar system at $T = 135$ K and $p = 40$ bar and in Table IV for the pure quadrupolar Kr system at the same simulation state point. The density, LJ and quadrupole–quadrupole contributions to the internal energy and the shear viscosity are reported as a function of strain rate (γ). The shear viscosity is shown as a

TABLE III The densities(ρ in g/cm^3), *LJ* and quadrupole–quadrupole energies(E_{LJ} and E_{QQ} in kJ/mole), and viscosities(η in 10^{-7} N s/m^2) of the pure quadrupolar argon system as a function of strain rate(γ in ps^{-1}) and quadrupole moment(Q in *B*) at $T = 135$ K and $p = 40$ bar. These units are used for density, energy, viscosity and quadrupole moment in all remaining tables

γ	*Run length*	ρ	$-E_{LJ}$	$-E_{QQ}$	η	ρ	$-E_{LJ}$	$-E_{QQ}$	η
		Quadrupolar Ar ($Q = 0.688$ B)				Quadrupolar Ar ($Q = 1.376$ B)			
1.0	60 k	0.850	3.336	0.007	520.8	0.900	3.526	0.110	538.3
0.81	60 k	0.904	3.599	0.007	576.1	0.951	3.766	0.131	584.4
0.64	60 k	0.973	3.882	0.010	640.8	1.013	4.025	0.140	664.2
0.49	100 k	1.015	4.091	0.010	693.7	1.051	4.223	0.154	725.8
0.36	100 k	1.041	4.215	0.010	733.8	1.072	4.317	0.162	807.9
0.25	100 k	1.046	4.244	0.010	771.4	1.088	4.401	0.163	853.2
0.16	160 k	1.057	4.292	0.012	814.5	1.089	4.409	0.163	933.8
0.09	160 k	1.060	4.312	0.012	842.9	1.092	4.419	0.163	985.5
0.04	200 k	1.062	4.321	0.012	892.1	1.092	4.412	0.165	1036
		Quadrupolar Ar ($Q = 2.063$ B)				Quadrupolar Ar ($Q = 2.751$ B)			
1.0	60 k	0.998	3.853	0.598	606.1	1.194	4.338	2.269	950.8
0.81	60 k	1.056	4.110	0.659	734.3	1.261	4.599	2.547	1150
0.64	60 k	1.136	4.456	0.771	851.0	1.313	4.823	2.671	1352
0.49	100 k	1.144	4.506	0.819	948.1	1.333	4.893	2.830	1481
0.36	100 k	1.178	4.661	0.859	1006	1.366	5.034	2.935	1645
0.25	100 k	1.194	4.735	0.895	1087	1.390	5.138	3.016	1818
0.16	160 k	1.206	4.791	0.891	1174	1.405	5.203	3.071	1970
0.09	160 k	1.211	4.810	0.902	1269	1.414	5.243	3.107	2147
0.04	200 k	1.215	4.830	0.919	1341	1.415	5.247	3.114	2441

TABLE IV The densities, *LJ* and quadrupole–quadrupole energies, and viscosities of the pure quadrupolar krypton system as a function of strain rate and quadrupole moment at $T = 135$ K and $p = 40$ bar. Units and symbols are defined in Table III

γ	*Runlength*	*Quadrupolar Kr* ($Q = 1.376$ *B*) ρ	$-E_{LJ}$	$-E_{QQ}$	η	*Quadrupolar Kr* ($Q = 2.751$ *B*) ρ	$-E_{LJ}$	$-E_{QQ}$	η
1.0	60 k	1.801	5.740	0.057	876.0	1.948	6.087	0.937	1075
0.81	60 k	1.946	6.299	0.073	1162	2.090	6.617	1.135	1379
0.64	60 k	2.057	6.761	0.096	1445	2.195	7.019	1.284	1751
0.49	100 k	2.154	7.168	0.098	1684	2.281	7.354	1.428	2117
0.36	100 k	2.214	7.430	0.101	1968	2.354	7.643	1.545	2462
0.25	100 k	2.262	7.627	0.107	2321	2.416	7.895	1.626	2868
0.16	160 k	2.299	7.795	0.118	2609	2.466	8.099	1.691	3260
0.09	160 k	2.319	7.880	0.121	2774	2.494	8.223	1.720	3508
0.04	200 k	2.346	7.999	0.123	3078	2.521	8.333	1.753	4172

function of $\gamma^{1/2}$ for the pure quadrupolar Ar in Figure 1 and for the pure quadrupolar Kr in Figure 2. The trend of the computed viscosities as a function of $\gamma^{1/2}$ for both pure quadrupolar systems is almost the same as

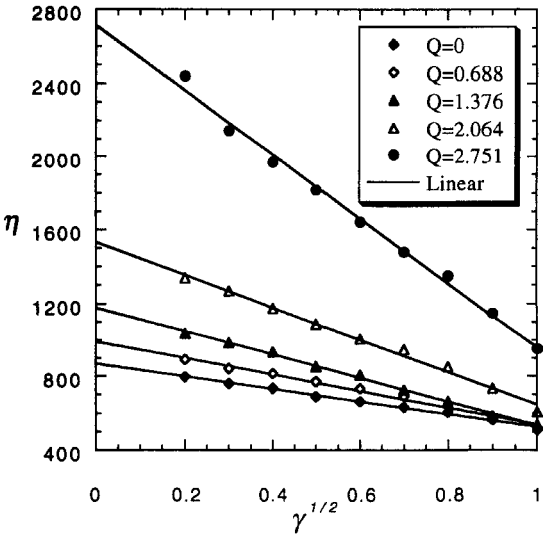

FIGURE 1 Shear viscosities (in units of 10^{-7} N·s/m^2) for pure quadrupolar Ar as a function of the square root of the strain rate (in units of ps$^{-1/2}$) at $T=135$ K and $p=40$ bar. The straight lines are least squared linear fits to the simulation results.

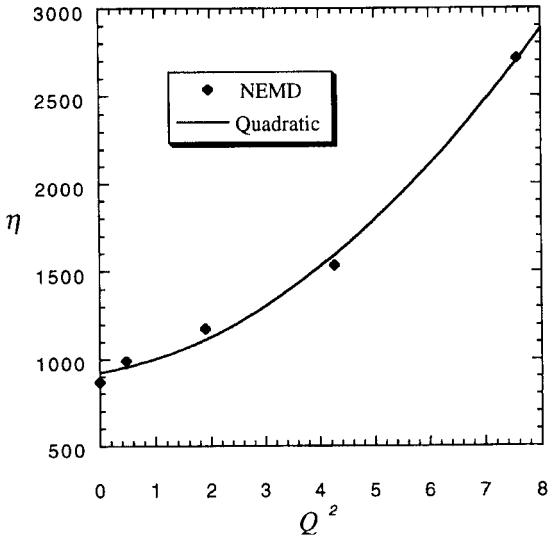

FIGURE 2 Shear viscosities (in units of 10^{-7} N·s/m^2) for pure quadrupolar Kr as a function of the square root of the strain rate (in units of ps$^{-1/2}$) at $T=135$ K and $p=40$ bar. The straight lines are least squared linear fits to the simulation results.

that for both pure dipolar systems [3]: the computed viscosities fit the theoretical relationship, Eq. (20), quite well, and the slopes of viscosities against $\gamma^{1/2}$ for the pure dipolar and quadrupolar Kr systems are much steeper than those for the pure corresponding Ar systems. These general features are also found in the nondipolar nonquadrupolar Ar and Kr systems [1] and the second feature is mainly due to the slopes of viscosities for the nondipolar nonquadrupolar Ar and Kr as shown in the cases of $Q=0$ in Figures 1 and 2. The zero strain rate extrapolations of the shear viscosity, shown as least-squares fitted straight lines in Figures 1 and 2, are used to determine the values of the shear viscosity which are reported in Table V for the pure quadrupolar Ar and Table VI for the pure quadrupolar Kr. Also presented in Tables V and VI are the density, and LJ and quadrupole–quadrupole energies as a function of quadrupole moment at $T=135\,\mathrm{K}$ and $p=40\,\mathrm{bar}$. The ratio (η/η_o) of the shear viscosity with nonzero quadrupole moment (η) to that with zero quadrupole moment (η_o) is also listed in Tables V and VI.

In the previous study of NEMD simulations for dipolar fluids [3], a dimensionless squared dipole moment was defined as

$$\mu^{*2} = \rho_N \mu^2 / \varepsilon, \tag{21}$$

where ρ_N is the number density and ε is the *LJ* energy parameter, and the ratio (η/η_o) of the shear viscosity with nonzero dipole moment (η) to that with zero dipole moment (η_o) was plotted as a function of the dimensionless

TABLE V The densities, *LJ* and quadrupole–quadrupole energies, and viscosities of the pure quadrupolar argon system as a function of quadrupole moment at $T=135\,\mathrm{K}$ and $p=40\,\mathrm{bar}$. Units and symbols are defined in Table III

System	Q	ρ	Q^{*2}	$-E_{LJ}$	$-E_{QQ}$	η	η/η_o
NpT MD	0.000	1.062	0.0000	4.321	0.000	885	1.000
NpT MD	0.688	1.073	0.0399	4.363	0.011	992	1.121
NpT MD	1.376	1.110	0.1652	4.506	0.170	1178	1.331
NpT MD	2.063	1.206	0.4034	4.791	0.901	1535	1.734
NpT MD	2.751	1.422	0.8459	5.280	3.119	2714	3.067

TABLE VI The densities, *LJ* and quadrupole–quadrupole energies, and viscosities of the pure quadrupolar krypton system as a function of quadrupole moment at $T=135\,\mathrm{K}$ and $p=40\,\mathrm{bar}$. Units and symbols are defined in Table III

System	Q	ρ	Q^{*2}	$-E_{LJ}$	$-E_{QQ}$	η	η/η_o
NpT MD	0.000	2.327	0.0000	7.945	0.000	3425	1.000
NpT MD	1.376	2.342	0.1046	7.987	0.120	3652	1.066
NpT MD	2.751	2.524	0.4511	8.343	1.780	4765	1.391

squared dipole moment. In this study, a dimensionless squared quadrupole moment is defined as

$$Q^{*2} = \rho_N Q^2 / \varepsilon\sigma^2 \tag{22}$$

where σ is the *LJ* length parameters. In Figure 3, the behavior of the shear viscosity as a function of Q^{*2} is shown. The viscosity is almost linear in Q^{*2} except for the largest value of Q^{*2} for the quadrupolar Ar system. The behavior of the shear viscosity ratio η/η_o as a function of Q^{*2} for both pure quadrupolar systems is also very similar to that of η/η_o as a function of μ^{*2} for both pure dipolar systems [3]: the linearity of η/η_o as a function of Q^{*2} and the difference in slope of η/η_o for quadrupolar Ar and Kr systems. The large slope in the case of quadrupolar Ar is probably due to the significant change of the density with increasing Q^{*2} in contrast with the small change of the density in the quadrupolar Kr as was observed in the cases of pure dipolar systems [3]. Tables V and VI show a 33.9% increase of the density for the quadrupolar Ar compared to a 8.5% increase for the quadrupolar Kr (a 39.3% increase for the dipolar Ar compared to a 14.6% increase for the dipolar Kr).

The results of pure dipolar quadrupolar Ar system at $T = 135\,\text{K}$ and $p = 40\,\text{bar}$ are summarized in Table VII. The density, *LJ*, dipole–dipole, dipole–quadrupole and quadrupole–quadrupole contributions to the internal energy and the shear viscosity are reported as a function of strain rate. The shear viscosity is shown as a function of $\gamma^{1/2}$ for the pure Ar, pure dipolar Ar, pure quadrupolar Ar and pure dipolar quadrupolar Ar systems

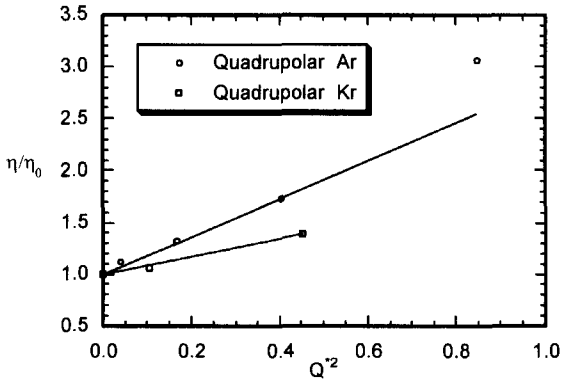

FIGURE 3 Ratio of Newtonian shear viscosities for pure quadrupolar Ar and Kr to the corresponding shear viscosity in the absence of quadrupolar interaction at $T = 135\,\text{K}$ and $p = 40\,\text{bar}$ as a function of the square of the reduced quadrupole moment.

TABLE VII The densities, *LJ*, dipole–dipole(E_{DD} in kJ/mole), dipole–quadrupole(E_{DQ} in kJ/mole) and quadrupole–quadrupole energies, and viscosities of the pure dipolar($\mu = 1.051$ D) quadrupolar($Q = 1.376$ B) argon system as a function of strain rate at $T = 135$ K and $p = 40$ bar. Other units and symbols are defined in Table III

γ	*Run length*	ρ	$-E_{LJ}$	$-E_{DD}$	$-E_{DQ}$	$-E_{QQ}$	η
1.0	60 k	1.135	4.288	1.377	0.548	0.053	836.5
0.81	60 k	1.173	4.472	1.463	0.598	0.063	962.8
0.64	60 k	1.225	4.705	1.545	0.640	0.073	1151
0.49	100 k	1.254	4.838	1.589	0.667	0.077	1220
0.36	100 k	1.277	4.952	1.618	0.695	0.080	1312
0.25	100 k	1.301	5.061	1.663	0.708	0.080	1460
0.16	160 k	1.314	5.123	1.691	0.714	0.082	1603
0.09	160 k	1.318	5.143	1.693	0.726	0.083	1638
0.04	200 k	1.321	5.153	1.698	0.734	0.084	1741
0.0	100 k	1.330	5.192	1.705	0.740	0.086	2004*

* Extrapolated at $\gamma = 0$ by least squared linear fits of the simulation results.

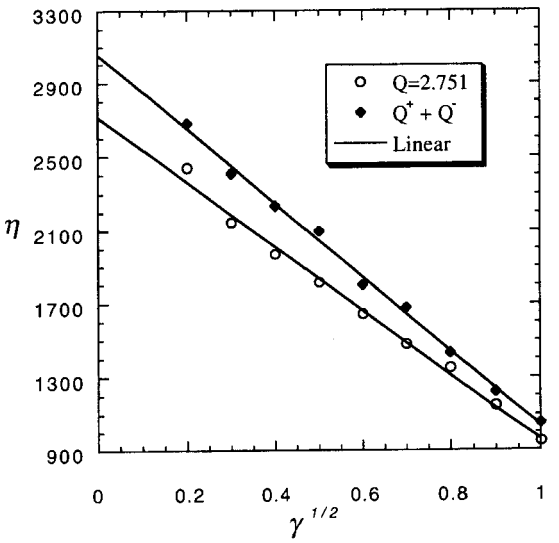

FIGURE 4 Shear viscosities (in units of 10^{-7} N·s/m^2) for pure Ar, pure quadrupolar Ar, pure dipolar Ar, and pure dipolar quadrupolar Ar, as a function of the square root of the strain rate (in units of ps$^{-1/2}$) at $T = 135$ K and $p = 40$ bar. The straight lines are least squared linear fits to the simulation results.

in Figure 4. Since the chosen magnitudes of dipolar moment (1.051 D) and quadrupolar moment (1.376 B) are of intermediate values, it is interesting to compare the changes in the viscosity, density, and energy as the system changes according to the order in the strength of the intermolecular potential – the pure Ar, pure quadrupolar Ar, pure dipolar Ar, and pure

dipolar quadrupolar Ar. First, in the viscosity change of 885, 1178, 1657, and 2004×10^{-7} Ns/m^2, the increase of the viscosity by adding the quadrupolar moment to the pure Ar is almost the same increase by adding the quadrupolar moment to the pure dipolar Ar. Second, the same trend is seen in the density change -1.062, 1.110, 1.256 and 1.330 g/cm^3, which reflects that the increase of the viscosity according to the order in the strength of the intermolecular potential is mainly due to the increase of density. Finally, the energy change is more complicated. The same trend is also seen in the *LJ* energy change (-4.321, -4.506, -4.957 and -5.192 kJ/mol). The quadrupole–quadrupole energy in the pure quadrupolar Ar is larger than that in the pure dipolar quadrupolar Ar (-0.170 *vs.* -0.086 kJ/mol), and similarly the dipole–dipole energy in the pure dipolar Ar is larger than that in the pure dipolar quadrupolar Ar (-1.932 *vs.* -1.705 kJ/mol), but the pure dipolar quadrupolar Ar is compensated by the dipole–quadrupole energy (-0.740 kJ/mol).

The next system we simulated is the mixture of two kinds of quadrupolar Ar of which halves have Q^+ and Q^- with $Q = 2.751$ B at $T = 135$ K and $p = 40$ bar. The density, *LJ* and quadrupole–quadrupole contributions to the internal energy and the shear viscosity are reported as a function of strain rate in Table VIII. The shear viscosity is shown as a function of $\gamma^{1/2}$ compared with that for the pure quadrupolar Ar in Figure 5. The large increase in the quadrupole–quadrupole energy (-4.035 *vs.* -3.119 kJ/mol) with the small decrease in the *LJ* energy (-5.219 *vs.* -5.280 kJ/mol) results in the large increase in the density (2.266 *vs.* 1.422 g/cm^3), and therefore the large increase in the viscosity (3057 *vs.* 2714×10^{-7} Ns/m^2). The large quadrupole–quadrupole energy in the mixture of two kinds of quadrupolar

TABLE VIII The densities, *LJ* and quadrupole–quadrupole energies, and viscosities of the mixture of two kinds of quadrupolar argon(halves of the system have Q^+ and Q^- with $Q = 2.751$ B) as a function of strain rate at $T = 135$ K and $p = 40$ bar. Units and symbols are defined in Table III

γ	*Run length*	ρ	$-E_{LJ}$	$-E_{QQ}$	η
1.0	60 k	1.890	4.304	2.844	1052
0.81	60 k	1.972	4.507	3.100	1223
0.64	60 k	2.040	4.674	3.301	1432
0.49	160 k	2.104	4.816	3.546	1678
0.36	160 k	2.156	4.937	3.714	1800
0.25	160 k	2.190	5.030	3.808	2098
0.16	160 k	2.224	5.123	3.867	2237
0.09	160 k	2.245	5.160	3.994	2409
0.04	200 k	2.259	5.198	4.022	2682
0.0	100 k	2.266	5.219	4.035	3057*

* Extrapolated at $\gamma = 0$ by least squared linear fits of the simulation results.

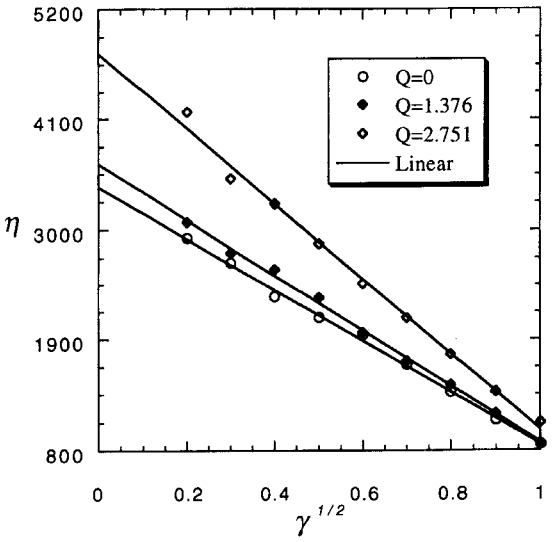

FIGURE 5 Shear viscosities (in units of 10^{-7} 2) for the mixture of pure quadrupolar Ar with Q^+ and $Q^-(Q=2.751\,\mathrm{B})$ as a function of the square root of the strain rate (in units of $\mathrm{ps}^{-1/2}$) at $T=135\,\mathrm{K}$ and $p=40\,\mathrm{bar}$. The straight lines are least squared linear fits to the simulation results.

Ar compared to the pure quadrupolar Ar with the same magnitude of quadrupole moment comes from the way how the quadrupole aligns itself with the nearest neighbor. The alignment of two different kinds of quadrupoles, Q^+ and Q^-, has a lower quadrupole–quadrupole energy than that of the same quadrupoles as demonstrated in the figure below.

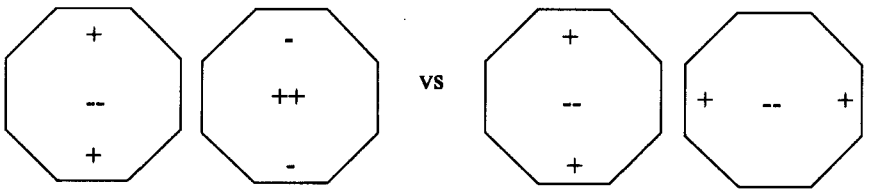

The strain rate dependent densities, LJ and quadrupole–quadrupole energies, and viscosities of two mixtures – nonquadrupolar Ar/quadrupolar Kr system ($Q_{\mathrm{Kr}}=2.751\,\mathrm{B}$, referred to as case B) and quadrupolar Ar/quadrupolar Kr ($Q_{\mathrm{Ar}}=1.376\,\mathrm{B}$ and $Q_{\mathrm{Kr}}=2.751\,\mathrm{B}$, referred to as case C) – are given in Tables IX and X increasing in steps of 1/6 in the quadrupolar Kr mole fraction x. The viscosities of both mixture systems are plotted as a function of square root of strain rate, $\gamma^{1/2}$, in Figures 6 and 7. As in the case

TABLE IX The densities, LJ and quadrupole–quadrupole energies, and viscosities of nonquadrupolar/quadrupolar mixture, nonquadrupolar Ar/quadrupolar Kr($Q = 2.751$ B) system (Case B), as a function of strain rate and quadrupolar Kr mole fraction x at $T = 135$ K and $p = 40$ bar. Units and symbols are defined in Table III

γ	*Run length*	ρ	$-E_{LJ}$	$-E_{QQ}$	η	ρ	$-E_{LJ}$	$-E_{QQ}$	η
			$x = 1/6$				$x = 1/3$		
1.0	60 k	1.062	3.914	0.032	582.1	1.272	4.457	0.110	646.9
0.81	60 k	1.148	4.285	0.042	675.8	1.342	4.750	0.112	787.1
0.64	60 k	1.205	4.529	0.030	778.4	1.422	5.093	0.157	943.9
0.49	100 k	1.257	4.754	0.045	880.7	1.469	5.300	0.167	1068
0.36	100 k	1.269	4.822	0.050	959.5	1.500	5.436	0.170	1198
0.25	100 k	1.286	4.898	0.043	1028	1.521	5.538	0.195	1272
0.16	160 k	1.306	4.995	0.053	1103	1.547	5.644	0.196	1390
0.09	160 k	1.332	5.108	0.044	1235	1.553	5.667	0.199	1499
0.04	200 k	1.347	5.180	0.051	1283	1.557	5.687	0.191	1632
			$x = 1/2$				$x = 2/3$		
1.0	60 k	1.438	4.826	0.247	745.6	1.629	5.326	0.430	857.2
0.81	60 k	1.543	5.250	0.279	935.4	1.720	5.679	0.506	1079
0.64	60 k	1.626	5.598	0.339	1127	1.831	6.130	0.584	1334
0.49	100 k	1.679	5.836	0.377	1307	1.893	6.384	0.643	1574
0.36	100 k	1.725	6.036	0.381	1470	1.953	6.638	0.718	1787
0.25	100 k	1.769	6.215	0.419	1596	1.992	6.795	0.733	2013
0.16	160 k	1.781	6.267	0.435	1740	2.016	6.904	0.761	2226
0.09	160 k	1.798	6.346	0.443	1906	2.024	6.943	0.764	2425
0.04	200 k	1.812	6.406	0.450	2109	2.040	7.010	0.781	2711
			$x = 5/6$						
1.0	60 k	1.781	5.675	0.664	963.6				
0.81	60 k	1.898	6.122	0.782	1243				
0.64	60 k	2.023	6.603	0.915	1524				
0.49	100 k	2.082	6.850	0.992	1801				
0.36	100 k	2.155	7.144	1.092	2063				
0.25	100 k	2.202	7.336	1.140	2373				
0.16	160 k	2.241	7.496	1.193	2636				
0.09	160 k	2.272	7.628	1.208	2922				
0.04	200 k	2.282	7.674	1.222	3395				

of both dipolar mixture systems [3], the computed viscosities for both quadrupolar systems fit the theoretical relationship, Eq. (20), quite well. The zero strain rate extrapolations of the shear viscosity, shown as least-squares fitted straight lines in Figures 6 and 7, are used to determine the values of the shear viscosity reported in Table XI for the nonquadrupolar/quadrupolar mixture and Table XII for the quadrupolar/quadrupolar mixture along with densities and energies as a function of mole fraction of quadrupolar Kr.

The composition dependent shear viscosities, total configurational energies and densities for the two mixtures (cases B and C) are shown in Figures 8–10 respectively along with the nonquadrupolar/nonquadrupolar

TABLE X The densities, LJ and quadrupole–quadrupole energies, and viscosities of quadrupolar/quadrupolar mixture, quadrupolar Ar($Q = 1.376$ B)/quadrupolar Kr($Q = 2.751$ B) system (Case C), as a function of strain rate and quadrupolar Kr mole fraction x at $T = 135$ K and $p = 40$ bar. Units and symbols are defined in Table III

γ	*Run length*	ρ	$-E_{LJ}$	$-E_{QQ}$	η	ρ	$-E_{LJ}$	$-E_{QQ}$	η
			$x = 1/6$				$x = 1/3$		
1.0	60 k	1.115	4.079	0.220	606.5	1.283	4.453	0.310	698.7
0.81	60 k	1.195	4.425	0.235	728.4	1.398	4.924	0.382	872.8
0.64	60 k	1.256	4.690	0.275	837.9	1.450	5.148	0.414	993.0
0.49	100 k	1.300	4.894	0.291	944.1	1.519	5.438	0.453	1161
0.36	100 k	1.321	4.988	0.303	1034	1.547	5.569	0.478	1316
0.25	100 k	1.337	5.060	0.310	1145	1.576	5.687	0.509	1426
0.16	160 k	1.358	5.161	0.315	1266	1.589	5.753	0.510	1544
0.09	160 k	1.361	5.180	0.317	1377	1.620	5.885	0.538	1658
0.04	200 k	1.367	5.200	0.334	1489	1.608	5.834	0.529	1858
			$x = 1/2$				$x = 2/3$		
1.0	60 k	1.485	4.975	0.456	813.5	1.655	5.379	0.620	922.4
0.81	60 k	1.573	5.327	0.531	983.5	1.755	5.774	0.694	1160
0.64	60 k	1.646	5.632	0.591	11162	1.839	6.110	0.815	1420
0.49	100 k	1.729	5.963	0.684	1408	1.936	6.526	0.975	1681
0.36	100 k	1.771	6.143	0.704	1567	1.982	6.719	1.007	1961
0.25	100 k	1.795	6.257	0.716	1702	2.026	6.875	1.020	2213
0.16	160 k	1.824	6.378	0.759	1863	2.045	6.964	1.026	2436
0.09	160 k	1.844	6.462	0.769	2092	2.074	7.076	1.068	2628
0.04	200 k	1.851	6.492	0.776	2351	2.089	7.148	1.056	2937
			$x = 5/6$						
1.0	60 k	1.766	5.606	0.736	1059				
0.81	60 k	1.934	6.259	1.003	1324				
0.64	60 k	2.006	6.523	1.015	1608				
0.49	100 k	2.110	6.948	1.226	1917				
0.36	100 k	2.177	7.212	1.275	2320				
0.25	100 k	2.224	7.388	1.287	2547				
0.16	160 k	2.263	7.547	1.347	2873				
0.09	160 k	2.287	7.652	1.383	3093				
0.04	200 k	2.308	7.741	1.392	3501				

mixture (case A) from Ref. [1]. For ideal liquid mixtures, the linear dependence of the properties on composition would be expected, *i.e.*,

$$P = x_1 P_1 + (1 - x_1) P_2 \tag{23}$$

where P is η, E, and the molar volume $\nu = 1/\rho_N N_A$ where N_A is Avogadro's number. From Figure 8 it is clear that the viscosities deviate significantly from this linear relationship. A common engineering correlation for liquid mixture viscosities is given by [16]

$$\eta = \exp[x_1 \ln \eta_1 + (1 - x_1) \ln \eta_2] \tag{24}$$

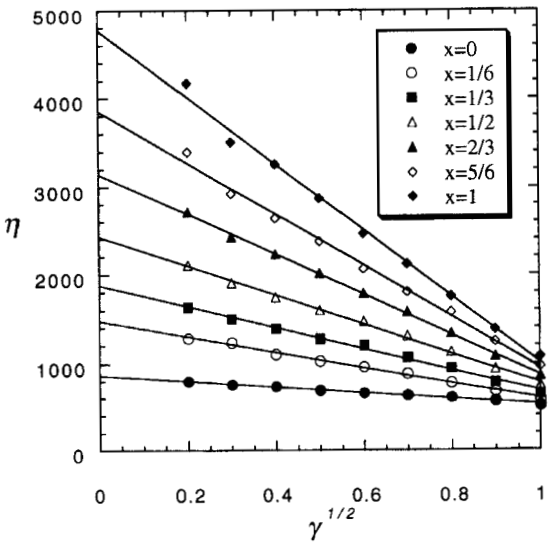

FIGURE 6 Strain rate dependence of the shear viscosities (in units of 10^{-7} N·s/m^2) for nonquadrupolar Ar/quadrupolar Kr (Case B) mixtures as a function of the square root of the strain rate (in units of ps$^{-1/2}$) and of quadrupolar Kr mole fraction at $T = 135$ K and $p = 40$ bar. The straight lines are least squared linear fits to the simulation results.

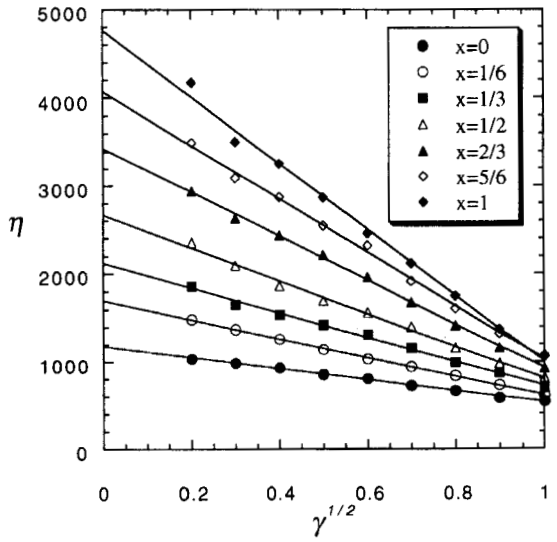

FIGURE 7 Strain rate dependence of the shear viscosities (in units of 10^{-7} N·s/m^2) for quadrupolar Ar/quadrupolar Kr (Case C) mixtures as a function of the square root of the strain rate (in units of ps$^{-1/2}$) and of quadrupolar Kr mole fraction at $T = 135$ K and $p = 40$ bar. The straight lines are least squared linear fits to the simulation results.

TABLE XI The densities, LJ and quadrupole–quadrupole energies, and viscosities of nonquadrupolar/quadrupolar mixture, nonquadrupolar Ar/quadrupolar Kr($Q = 2.751$ B) system (Case B), as a function of quadrupolar Kr mole fraction x at $T = 135$ K and $p = 40$ bar. Units and symbols are defined in Table III

x	ρ	$-E_{LJ}$	$-E_{QQ}$	η
0	1.062	4.321	0.0	885
1/6	1.305	4.999	0.047	1475
1/3	1.555	5.686	0.182	1877
1/2	1.808	6.386	0.495	2425
2/3	2.057	7.075	0.782	3146
5/6	2.293	7.724	1.220	3854
1	2.524	8.343	1.780	4765

TABLE XII The densities, LJ and quadrupole–quadrupole energies, and viscosities of quadrupolar/quadrupolar mixture, quadrupolar Ar($Q = 1.376$ B)/quadrupolar Kr($Q = 2.751$ B) system (Case C), as a function of quadrupolar Kr mole fraction x at $T = 135$ K and $p = 40$ bar. Units and symbols are defined in Table III

x	ρ	$-E_{LJ}$	$-E_{QQ}$	η
0	1.110	4.506	0.170	1178
1/6	1.361	5.183	0.319	1701
1/3	1.602	5.817	0.571	2117
1/2	1.854	6.502	0.789	2666
2/3	2.088	7.138	1.064	3431
5/6	2.308	7.737	1.444	4073
1	2.524	8.343	1.780	4765

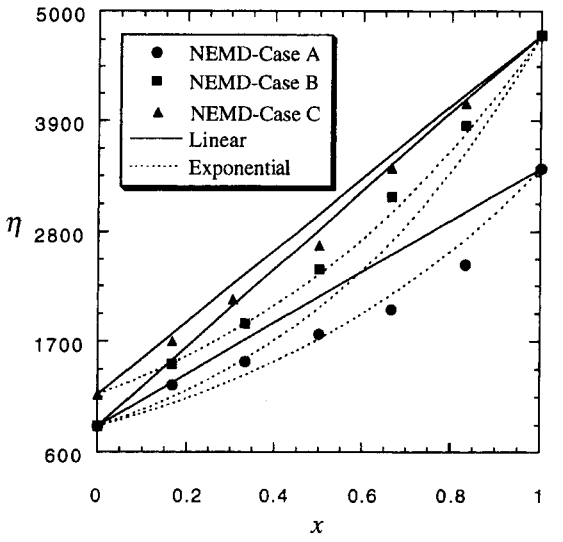

FIGURE 8 Composition dependence of the shear viscosity of Ar/Kr mixtures (A: nonquadrupolar/nonquadrupolar, B: nonquadrupolar/quadrupolar, C: quadrupolar/quadrupolar). In each case, the straight line is the linear dependence expected in the case of ideal liquid mixtures and the dashed line is the exponential model given by Eq. (23) of the text.

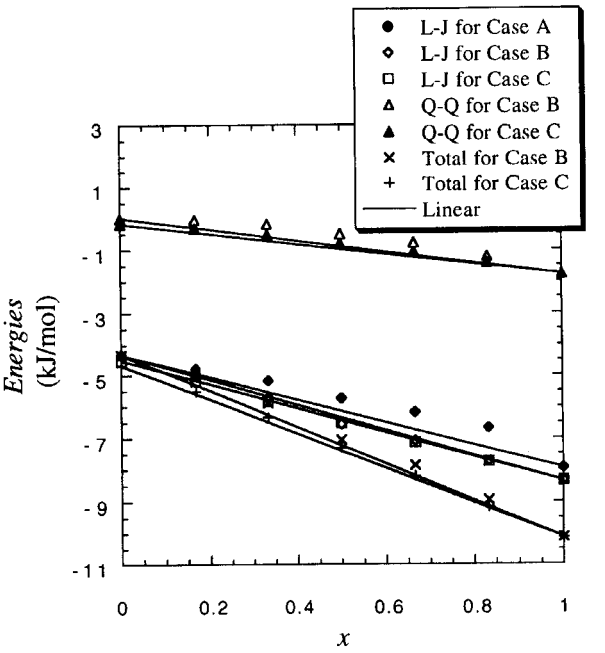

FIGURE 9 Composition dependence of the total energies, E_{LJ} and E_{QQ} of Ar/Kr mixtures (A: nonquadrupolar/nonquadrupolar, B: nonquadrupolar/quadrupolar, C: quadrupolar/quadrupolar). In each case, the straight line is the linear dependence expected in the case of ideal liquid mixtures.

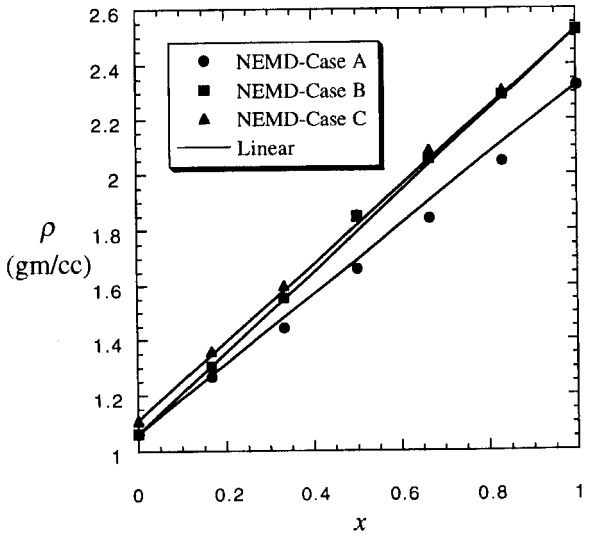

FIGURE 10 Composition dependence of the density of Ar/Kr mixtures (A: nonquadrupolar/nonquadrupolar, B: nonquadrupolar/quadrupolar, C: quadrupolar/quadrupolar). In each case, the straight line is the linear dependence expected in the case of ideal liquid mixtures.

The dashed curves in Figure 8 represent the prediction of Eq. (24). The viscosities also deviate from the logarithmic relationship. In the cases of dipolar mixtures, the viscosities deviate from both predictions. The degree of deviations is very similar in the cases of quadrupolar mixtures and dipolar mixtures.

The LJ, quadrupole–quadrupole, and total energies for each case are shown in Figure 9 as a function of the quadrupolar Kr mole fraction x. There is only one energy (LJ) in case A. The linear composition dependence of the LJ parts of the energy is quite accurate for both nonquadrupolar/quadrupolar (case B) and quadrupolar/quadrupolar (case C) mixtures, while it is most inaccurate at the high Kr mole fraction end for the nonquadrupolar/quadrupolar mixture (case A) and hence for the total energy of case A. The quadrupole–quadrupole parts of the energy are linear for both cases B and C, but the linearity of case C is better than that of case B since quadrupolar/quadrupolar mixtures are generally more ideal than nonquadrupolar/quadrupolar mixtures. The total energies are also linear for both case B and case C, and the linearity of case C is better than that of cases B since the difference of the linearity for quadrupolar mixtures comes from the quadrupole–quadrupole part not the LJ part.

The mixture densities are shown in Figure 10 for the three cases along with the ideal liquid mixture prediction obtained by converting the linear expression for molar volume for an ideal liquid mixture, Eq. (23) with $P=\nu$, into densities in g/cc. Both the nonquadrupolar/quadrupolar mixture (case B) and quadrupolar/quadrupolar (case C) are described accurately by the ideal liquid mixture expression while the nonquadrupolar/nonquadrupolar mixture (case A) is not. This is consistent with the fact that the linearity of the total energies for both cases B and C is better than that of case A, but is not consistent with the idea that in the cases of the dipolar mixtures [3], dipolar/dipolar and nondipolar/nondipolar mixtures are likely to be more ideal than nondipolar/dipolar mixtures. This is mainly due to the weaker interaction of quadrupole–quadrupole than that of dipole–dipole.

IV. CONCLUSION

It is evident from all the results presented in this paper that, the addition of quadrupolar interactions to the pure Ar and the addition of quadrupolar interactions to the pure dipolar Ar, leads to higher viscosities as was observed in the addition of dipolar interactions [3] to the pure Ar. This could be so for two reasons. First, one might conjecture that the additional

attraction introduced by the quadrupole–quadrupole interaction has the same effect thermodynamically as decreasing temperature, which itself could lead to higher viscosities since liquid viscosity increases with decreasing temperature. Second, at constant pressure, the addition of the attractive quadrupole–quadrupole interaction results in the system moving to higher density to maintain the same pressure, and this density increase will also contribute to the increased viscosity.

From the results of NEMD for two mixtures – nonquadrupolar Ar/quadrupolar Kr system (case B) and quadrupolar Ar/quadrupolar Kr (case C), the viscosities of both mixture systems deviate from the linear and logarithmic dependence on the quadrupolar Kr mole fraction x as in the cases of dipolar mixtures. The total energies show a linear dependence for both cases B and C, and the linearity of case C is better than that of case B since the difference of the linearity for quadrupolar mixtures comes from the quadrupole–quadrupole part not from the LJ part. The mixture density for both cases B and C are described accurately by the ideal liquid mixture expression while the nonquadrupolar/nonquadrupolar mixture (case A) is not. This is not consistent with the idea that in the cases of the dipolar mixtures [3], dipolar/dipolar and nondipolar/nondipolar mixture are likely to be more ideal than nondipolar/dipolar mixtures. This is mainly due to the weaker interaction of quadrupole–quadrupole than that of dipole–dipole.

In future work, we will investigate the effect of nonlinear shape on the shear viscosity of pure fluids and their mixtures.

Acknowledgments

SHL thanks the Tongmyung University of Information Technology (Pusan, South Korea) for access to its IBM SP/2 computer. The work of PTC was supported by the Division of Chemical Sciences, Office of Basic Energy Sciences, U. S. Department of Energy.

References

[1] Lee, S. H. and Cummings, P. T. (1993). "Shear viscosity of model mixtures by non-equilibrium molecular dynamics. I. Argon–krypton mixtures", *J. Chem. Phys.*, **99**, 3919.

[2] Lee, S. H. and Cummings, P. T. (1994). "Shear viscosity of model mixtures by non-equilibrium molecular dynamics. II. Effect of dipolar interaction", *J. Chem. Phys.*, **101**, 6206.

[3] Lee, S. H. and Cummings, P. T. (1996). "Effect of three-body forces on the viscosity of liquid argon", *J. Chem. Phys.*, **105**, 2044.

[4] Barker, J. A., Fisher, R. A. and Watts, R. O. (1971). "Liquid argon: Monte Carlo and molecular dynamics calculations", *Mol. Phys.*, **21**, 657.

[5] Barker, J. A., Watts, R. O., Lee, J. K., Schafer, T. P. and Lee, Y. T. (1974). "Interatomic potentials for krypton and xenon", *J. Chem. Phys.*, **61**, 3081.
[6] Allen, M. P. and Tildesley, D. J., *Computer Simulation of Liquids* (Oxford University, Oxford, 1987), p. 334.
[7] Allen, M. P. and Tildesley, D. J., *Computer Simulation of Liquids* (Oxford University, Oxford, 1987), p. 332.
[8] Evans, D. J. (1977). "On the representation of orientation space", *Mol. Phys.*, **34**, 317.
[9] Evans, D. J. and Murad, S. (1977). "Singularity free algorithm for molecular dynamics simulation of simulation of rigid polyatomics", *Mol. Phys.*, **34**, 327.
[10] Hood, L. M., Evans, D. J. and Morriss, G. P. (1989). "Properties of a soft-sphere liquid from non-Newtonian molecular dynamics", *J. Stat. Phys.*, **57**, 729.
[11] Lees, A. W. and Edwards, S. F. (1972). "The computer study of transport processes under extreme conditions", *J. Phys. C: Solid State*, **5**, 1921.
[12] Evans, D. J. and Morriss, G. P. (1984). "Nonlinear response theory for steady planar Couette flow", *Phys. Rev.*, **A30**, 1528.
[13] Yamada, T. and Kawasaki, K. (1975). "Application of mode-coupling theory to nonlinear stress tensor in fluids", *Prog. Theor. Phys.*, **53**, 111.
[14] Kawasaki, K. and Gunton, J. D. (1973). "Theory of nonlinear transport processes: Nonlinear shear viscosity and normal stress effects", *Phys. Rev.*, **A8**, 2048.
[15] Ernst, M. H., Cichocki, B., Dorfman, J. R., Sharma, J. and van Beijeren, H. (1978). "Kinetic theory of nonlinear viscous flow in two and three dimensions", *J. Stat. Phys.*, **18**, 237.
[16] Reid, R. C., Prausnitz, J. M. and Sherwood, T. K., *The Properties and Liquids and Gases* (McGraw-Hill, New York, 1977), 3rd edn.